

<https://doi.org/10.15407/mineraljournal.40.04.053>  
UDC 549.642.2/4

**N.G. Yurchenko, M.M. Taran**

M.P. Semenenko Institute of Geochemistry, Mineralogy  
and Ore Formation of the NAS of Ukraine  
34, Acad. Palladin Ave., Kyiv, Ukraine, 03142  
E-mail: nadysya88@gmail.com, m\_taran@hotmail.com

## OPTICAL SPECTROSCOPIC AND COLORIMETRIC STUDY OF PYROXENES FROM FENITIZED ROCKS OF THE CHERNIHIVKA CARBONATITE MASSIF OF THE AZOV REGION

---

At exploration of carbonatite complexes the main attention is usually paid to investigation of the carbonatites themselves and various silicate magmatic rocks related to them, whilst much less attention is paid to the rocks of fenitized halos, which always accompany the carbonatite complexes being a powerful searching criterion. To expand instruments of forecasting and searching of carbonatites within the Ukrainian Shield, the influence of alkaline fenitizing fluids on optical spectroscopic parameters and coloration of rock-forming minerals was investigated. In this work the results of optical spectroscopy and colorimetric investigation of pyroxenes from metasomatically altered clinopyroxenites, crystalline schists, pyroxene containing migmatites of granite, tonalite and granosyenite compositions, syenites and alkaline syenites of fenitized halo of the northern part of Chernihivka carbonatite massif and its gneiss-migmatite frame host rocks are presented. It was found that spectroscopic features, color and pleochroism of the pyroxenes are caused by presence and ratio of different-valence iron ions,  $Fe^{2+}$  and  $Fe^{3+}$ , in the crystal structure, that causes appearance as crystal field absorption bands (bands of electronic dd-transitions), as the bands of intervalence charge-transfer  $Fe^{2+} \rightarrow Fe^{3+}$ . It is revealed that in the pyroxenes studied the M2 structural site is nearly completely filled by calcium and sodium ions, whereas  $Fe^{2+}$  are predominantly concentrated in the structural cationic positions M1. Nevertheless, even relatively low fraction of  $Fe^{2+}$  (M2)-ions significantly influences on the character of optical absorption in the near infrared range. By colorimetric investigations of grains of pyroxene from various rocks of the halo of fenitization the different character of coloration and its saturation, caused by different iron content and different degree of oxidation, is established.

*Keywords:* Ukrainian Shield, Chernihivka carbonatite massif, fenite halo, pyroxenes, optical spectroscopy, colorimetric study.

**Introduction.** Optical absorption spectra of transition metal ions in oxygen-based minerals, which provide a unique information on valence state, coordination, interatomic M-O distances, symmetry and constituents of ligand surrounding and other characteristics of such ions in mineral structures [19, 14], were object of numerous investigations. Particularly, the spectra of natural pyroxenes of different compositions have been intensively studied by e. g. Rossman [22, 23], Khomenko and Platonov [10], Khomenko [9], Burns [16] and many other investigators, especially those dealing with remote sensing exploration of celestial bodies of solar system [27, 18, 19]. According to X-ray diffraction studies [17] there are two types of

cationic positions M1 and M2 in the clinopyroxene structure which may accommodate  $Fe^{2+}$  ions (Fig. 1). Nominally, larger and more distorted M2-site is almost completely filled with  $Ca^{2+}$  and alkaline ions, so that  $Fe^{2+}$  is predominantly concentrated in the position M1, which at interpretation of optical spectra of pyroxenes is usually considered as an almost regular octahedron [20, 29]. Nevertheless, because of low symmetry and strong distortion of M2-position, intensities of the spin-allowed bands of  $Fe^{2+}$  (M2) in optical spectra of pyroxenes are frequently appreciably higher than that of  $Fe^{2+}$  (M1). Thus, in spectra of iron-bearing calcic clinopyroxenes the main spectroscopic features are caused by electronic spin-allowed dd-transitions of  $Fe^{2+}$  distributed between two non-equivalent cationic positions M1 and M2. They

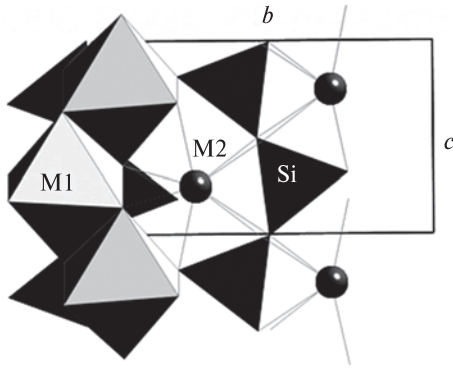


Fig. 1. A fragment of the diopside crystal structure (projection along the axis *a*). Silicon-oxygen tetrahedrons form infinite zigzag chains stretched along the crystallographic axis *c*. The structural position M1 is looking like a slightly distorted octahedron. The M2 position is larger in size and more distorted. In addition, it changes its coordination number depending on the size M2-cation. M1 and M2 polyhedra, which accommodate Fe<sup>2+</sup> and Fe<sup>3+</sup>, are connected by common edges and this leads to appearance of Fe<sup>2+</sup> → Fe<sup>3+</sup> IVCT bands in the pyroxenes optical spectra

cause two pairs of broad intense absorption bands in near-infrared (NIR) range from ca. 12.000 to 8.000 cm<sup>-1</sup>. Traces of Fe<sup>3+</sup> ions are responsible for an additional broad band located between 12.000 cm<sup>-1</sup> and 14.000 cm<sup>-1</sup> and caused by electronic Fe<sup>2+</sup> → Fe<sup>3+</sup> intervalence charge-transfer (IVCT) transition between ferrous and ferric ions in adjacent edge-shared M1 octahedra of the structure [15]. Besides, admixture of Fe<sup>3+</sup> causes a significant intensification of the aforementioned spin-allowed dd-transitions of Fe<sup>2+</sup> due to electronic exchange-couple interaction with neighboring Fe<sup>3+</sup> ions. This phenomenon is known not only in clinopyroxenes, but in many other Fe<sup>2+</sup>, Fe<sup>3+</sup>-bearing minerals [15, 25, 26]. Tails of very intense UV ligand-metal charge transfer bands of O<sup>2-</sup> → Fe<sup>3+</sup> and O<sup>2-</sup> → Fe<sup>2+</sup> type cause a high-energy absorption edge, which usually extends the visible range and influences on coloration of pyroxenes. Also, as was recently established on synthetic Ti-doped diopsides [24], a certain effect on spectra

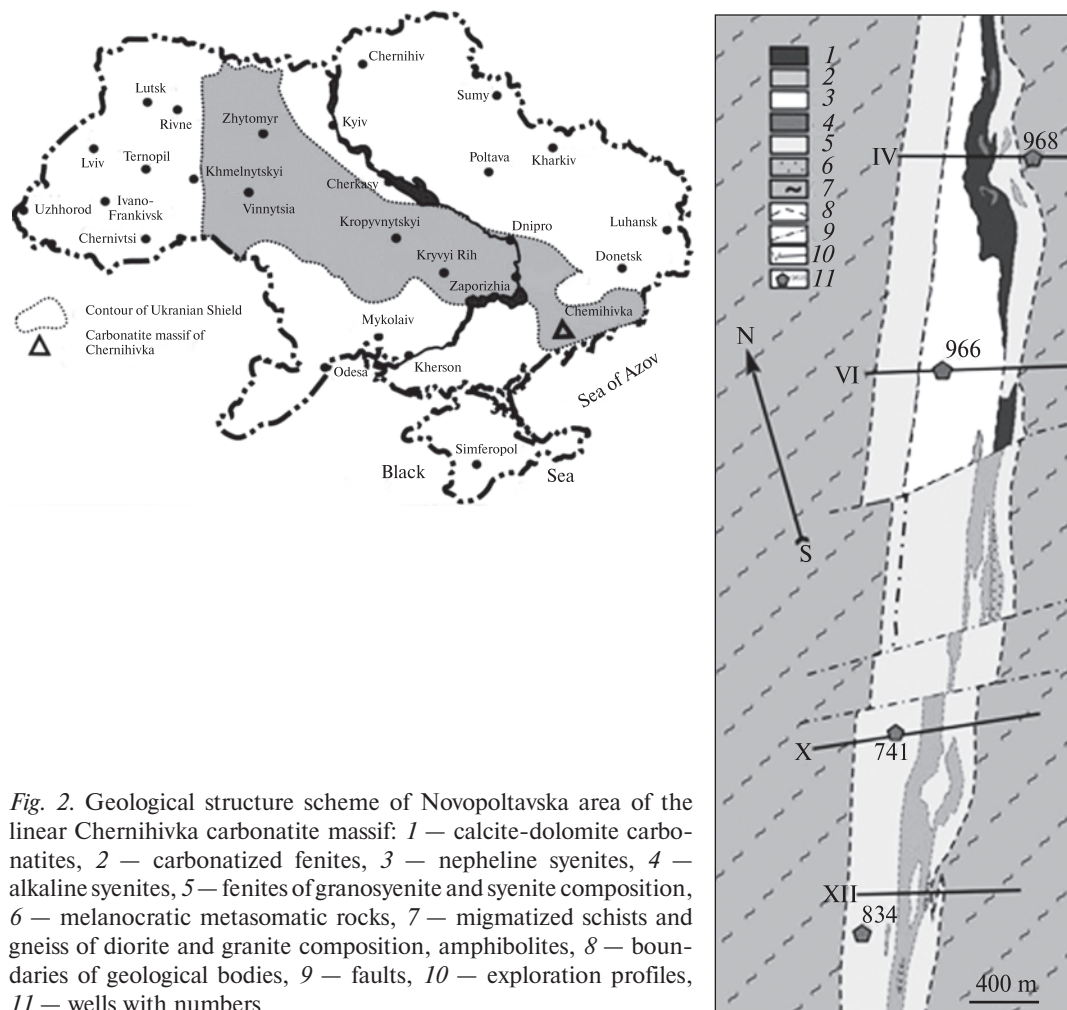


Fig. 2. Geological structure scheme of Novopoltavska area of the linear Chernihivka carbonatite massif: 1 – calcite-dolomite carbonatites, 2 – carbonatized fenites, 3 – nepheline syenites, 4 – alkaline syenites, 5 – fenites of granosyenite and syenite composition, 6 – melanocratic metasomatic rocks, 7 – migmatized schists and gneiss of diorite and granite composition, amphibolites, 8 – boundaries of geological bodies, 9 – faults, 10 – exploration profiles, 11 – wells with numbers

**Table 1. Morphological properties, color and pleochroism of investigated pyroxenes, their content and mineral paragenesis. Here and further in the paper a general pyroxene samples' number format is well/depth-grain number**

Sample	Pyroxene type, rock	Grains' shape, size, distribution character through the rock	Coloration in unpolarized light	Pleochroism and absorption scheme	Content in the rock, up to %	Mineral association	Secondary processes
834/250.4 <sup>1</sup>	Hedenbergite, apatite-containing clinopyroxenite	Xenomorphous prismatic; up to 5.0 mm long, forms aggregations of grains up to 10 mm in diameter	Green-yellow-green	Z – light green; X – green; Y – light brownish. X > Z ≈ Y	84	Albite, titanite, apatite, calcite	Rock albitization
741/243.0 <sup>2</sup>	Diopside, fenitized syenite	Xenomorphous, short prismatic, 0.3–0.8 mm, forms chains	Green	Z – light green; X – light green; Y – light brownish. X = Z ≈ Y	38	Titanite, biotite, magnetite	Replacement of pyroxene by colorless amphibole and calcite
741/246.0 <sup>3</sup>	Augite, clinopyroxenite	Prismatic, short prismatic, 0.5–3.0 mm, forms a solid prismatic-grained aggregation	Green	Z – light brownish-green; X – green; Y – light brownish. X > Z ≈ Y	91	Titanite, biotite, magnetite	Replacement of pyroxene by colorless amphibole and biotite
741/278.5 <sup>4</sup>	Aluminian augite, fenitized syenite	Short prismatic, 0.15–0.70 mm long, unevenly distributed in the rock, forms aggregations of small grains	Green	Z – yellow-green; X – green; Y – light brownish. X > Z > Y	24	Albite, titanite, apatite	Rock albitization, amphibolization and biotitization
741/287.0 <sup>5</sup>	Sodian augite (ferrian to aluminian), fenitized migmatites	Prismatic, short prismatic with an oval outline, in aggregations – granulated, 0.15–1.5 mm long, forms chains of grains	Green	Z – yellowish green; X – green; Y – light brownish. X > Z > Y	15	Albite - oligoclase, amphibole, biotite, magnetite, apatite	Pyroxene amphibolization and biotitization
741/306.9 <sup>6</sup>	Aluminian sodian augite, fenite	Prismatic, long prismatic, "sieve-like", with an oval outline; 0.16–2.0 mm long, linear chains with amphibole that replaces pyroxene	Green	Z – light green; X – green; Y – green. X ≈ Y > Z	6	Albite, alkaline amphibole, phlogopite	Rock amphibolization and albitization
966/573.0 <sup>7</sup>	Sodian diopside, fenite after biotite-pyroxene migmatites	Prismatic crystals from isometric to elongated habitus with poikilitic texture, outlines rounded, 0.5–7.0 mm long; layered, oriented	Light green	Z – light yellow-green; X – light green; Y – almost colorless, greenish. Z ≈ X > Y	34	Albite, biotite	Plagioclase albitization
968/453.8 <sup>8</sup>	Ferrian diopside, clinopyroxene-amphibole migmatite of granite composition	Randomly oriented short prismatic crystals with angular outlines, up to 1.0 mm long. Evenly distributed over the thin section area	Light green, almost colorless	Z – light green; X – colorless; Y – almost colorless; greenish. Z > Y > X	16	Quartz, oligoclase, microcline, amphibole, biotite, titanite, magnetite	Rock microclinization, replacement of pyroxene by blue-green amphibole and densely green amphibole

Sample	Pyroxene type, rock	Grains' shape, size, distribution character through the rock	Coloration in unpolarized light	Pleochroism and absorption scheme	Content in the rock, up to %	Mineral association	Secondary processes
968/466.0 <sup>9</sup>	Ferrian augite (augite-diopside), migmatite of tonalite composition	Randomly oriented short prismatic crystals with angular outlines, up to 1.0 mm long. Unevenly distributed over the thin section area	Light green, almost colorless	Z – light green; X – colorless; Y – almost colorless, greenish. Z > Y > X	8	Quartz, oligoclase, microcline, amphibole, biotite, titanite, magnetite	Plagioclase microclinization, slight replacement of individual pyroxene grains by brown biotite and almost colorless amphibole
968/472.0 <sup>10</sup>	Augite, migmatite of granosyenite composition	Randomly oriented short prismatic crystals with angular outlines, up to 1.2 mm long. Unevenly distributed over the thin section area	Light green, almost colorless	Z – light green; X – colorless; Y – almost colorless, greenish. Z > Y > X	14	Quartz, microcline, oligoclase, amphibole, biotite, titanite, magnetite	Microclinization, replacement of pyroxene by blue-green occasionally by green amphibole

Note. 1 – hedenbergite from apatite-containing clinopyroxenite; 2 – diopside from fenitized syenite; 3 – augite from clinopyroxenite; 4 – aluminian augite from fenitized syenite; 5 – sodian augite (from ferrian to aluminian) from fenitized migmatites; 6 – aluminian sodian augite from fenite; 7 – sodian diopside from fenite after biotite-pyroxene migmatites; 8 – ferrian diopside from clinopyroxene-amphibole migmatite of granite composition; 9 – ferrian augite (augite-diopside) from migmatite of tonalite composition; 10 – augite from migmatite of granosyenite composition.

Table 2. Values of formula coefficients for mineral forming components of pyroxenes from rocks of Chernihivka carbonatite complex Novopoltavska area

Sample number	Formula coefficients for mineral forming components											
	Si	Ti	Al (T)	Al (M1)	Fe <sup>3+</sup>	Fe <sup>2+</sup>	Mg	Mn	Ca	Na	K	Σ
834/250.4-1 <sup>1</sup>	1.970	0.002	0.029	0.017	0.093	0.451	0.450	0.026	0.879	0.080	0.003	4.000
741/246.0 <sup>2</sup>	1.949	0.018	0.051	0.048	0.003	0.316	0.657	0.022	0.913	0.000	0.024	4.001
741/278.5 <sup>3</sup>	2.037	0.030	0.000	0.105	0.000	0.540	0.446	0.016	0.777	0.025	0.025	4.001
741/287.0-1 <sup>4</sup>	1.951	0.004	0.056	0.038	0.134	0.263	0.709	0.014	0.685	0.139	0.009	4.002
741/287.0-2 <sup>5</sup>	1.980	0.009	0.020	0.114	0.040	0.386	0.556	0.012	0.732	0.148	0.003	4.000
741/306.9 <sup>6</sup>	2.029	0.019	0.000	0.086	0.042	0.460	0.502	0.010	0.627	0.220	0.004	3.999
966/573.0-1 <sup>7</sup>	1.992	0.000	0.008	0.094	0.014	0.333	0.630	0.009	0.818	0.099	0.002	3.999
966/573.0-2 <sup>8</sup>	1.990	0.000	0.010	0.073	0.036	0.295	0.659	0.013	0.825	0.094	0.004	3.999
968/453.8 <sup>9</sup>	1.915	0.000	0.061	0.000	0.152	0.181	0.796	0.014	0.836	0.042	0.004	4.001
968/466.0 <sup>10</sup>	1.861	0.000	0.083	0.000	0.235	0.097	0.788	0.029	0.866	0.033	0.008	4.000
968/472.0 <sup>11</sup>	1.980	0.000	0.020	0.056	M1-0.003	0.311	0.733	0.018	0.850	0.024	0.005	4.000

Note. 1 – hedenbergite, 2 – augite, 3 – aluminian augite, 4 – ferrian, sodian augite, 5 – aluminian, sodian augite, 6 – aluminian sodian augite, 7, 8 – sodian diopside, 9 – ferrian diopside, 10 – ferrian augite (augite-diopside), 11 – augite.

configuration may play E||Y-polarized IVCT band of VI Ti<sup>3+</sup> → IV Ti<sup>4+</sup> type.

The spectroscopic features of different types, related to transition metal ions, or 3d<sup>N</sup>-ions [21, 16], cause such important psycho-physical cha-

racteristics of minerals and compounds as color and pleochroism. Color and pleochroism of ferromagnesian silicates, mainly such as biotite, pyroxene and amphibole, or so-named mafic minerals, are regarded as important diagnostic and typo-

morphic features of rocks of many types. It is quite natural, therefore, that since seventies of the last century one of the important components of exploration of such minerals, besides of their microprobe composition determinations, structure refinements and various spectroscopic studies, were calculations of objective color characteristics in the CIE colorimetric system [3] of oriented self-supporting polished platelets or grains in petrographic thin sections. Presentation of such colorimetric parameters in forms of color fields, "vectors" of pleochroism etc. was broadly used by Ukrainian mineral spectroscopists for various genetic constructions and correlations [4, 10], as well as for instrumental measuring and description of colors of gems [6]. Colorimetric calculations and quantification of color and pleochroism of minerals by such quantities as the chromaticity coordinates  $x$ ,  $y$  and  $z$ , the dominant wavelength  $\lambda_k$ , dominant color purity or color saturation  $p_c$  and luminance  $Y$  of mafic minerals are still used nowadays for such purposes [8].

In this paper the results of exploration of clinopyroxenes from crystalline rocks of Novopoltavska area of the West Pre-Azov Region Chernihivka tectonic zone, where of the same name carbonatite complex is located (Fig. 2), represent another attempt of using optical absorption spectroscopy and colorimetric characteristics of mafic minerals in petrographic thin sections for correlation constructions and genetic interpretation of experimental data.

The distribution of carbonatite complex rocks within Novopoltavska area is controlled by NW-trending fault zone from settlement Chernihivka on the south till crossing with Konkskiy fault on the north. The host rocks are amphibole- and pyroxene-containing schists and plagiogneisses, which are interbedded with biotite plagiogneisses, granitized and migmatized in varying degrees, and belong to Lozovatska Suite of Zakhidnopryazovska Series. The complex had been forming for the period from 2190 to 1900 Ma with repeated activation of the process [12]. Some researchers attribute this complex to linear-fractured type for its tectonic position and character of distribution, although others consider it as a central-type formation [7].

It is considered [1, 13] that the most ancient formations of Chernihivka complex are alkaline ultramafic rocks and gabbroids, later on nepheline and alkaline syenites had been formed, whereas the youngest rocks are carbonatites (sovite, alvikite, beforosite [1]) that constitute dykes in the earlier

rocks and contain xenoliths of the latter. All alkaline rocks of the massif produce fenitization halo in host rocks and their remnants as a result of alkaline orcalcium-magnesium-ferruginousmetasomatism.

Novopoltavska area, located in the northern part of Chernihivka carbonatite massif, is composed of tectonically transformed metamorphic, ultrahigh-pressure metamorphic and intrusive rocks which were being influenced by metasomatic processes and contact metamorphic transformations during its formation. Here we represent the results of optical spectroscopic and colorimetric study of pyroxenes from crystalline schists, recrystallized dioritoides, pyroxene containing migmatites, syenites and alkaline syenites in the cores of drilled wells numbered 741, 834, 966 and 968, which were at our disposal. Their crystal optical properties and mineral associations are presented in Table 1. According to the results of the microprobe composition investigation by semi-quantitative EDS method [14] the pyroxenes studied can be assigned to augites, diopsides and their varieties such as sodium augites and diopsides, aluminium-iron augites, iron diopsides, magnesium hedenbergites and aluminian sodian augites. As seen from the Table 2, the main chromophore (transition metal) constituent in them is iron. The influence of other transition metals as Cr, Mn, Ti etc., which could have contributed to absorption spectra and colorimetric characteristics of natural clinopyroxenes [10, 28, 24], is negligible, although some weak contributions to the shape of spectral curves and thus to color and colorimetric parameters of pyroxenes cannot be completely excluded.

As known, investigations of carbonatite complexes are usually focused on mineralogical, petrographic and geochemical features of carbonatites themselves and associated magmatic formations. The fenitization halos (i.e. the metasomatically changed enclosing rocks), which always accompany carbonatite complexes and frequently have much broader distribution areas than the carbonatites themselves and their associated rocks, are much poorer studied [5, 14]. It seems reasonable that together with the traditional methods of investigations the expansion of forecasting and searching facilities for carbonatites should include detailed studies of their fenitization halo rocks by optical spectroscopic and colorimetric methods. To our knowledge pyroxenes from the rocks of this massif have not been yet studied in this way.

**Methods and samples.** The composition of pyroxenes was determined on scanning electron

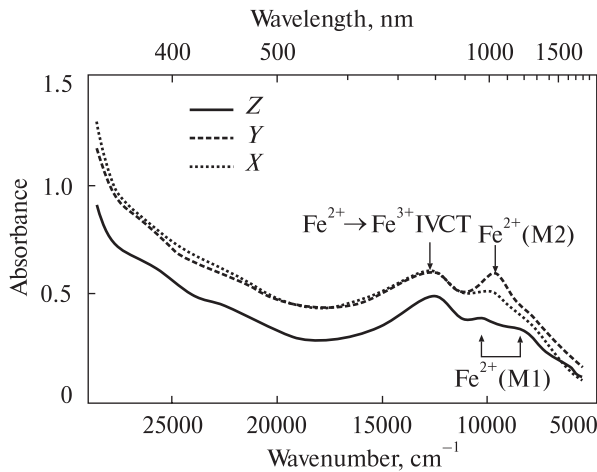


Fig. 3. Polarized absorption spectra of clinopyroxene augite-diopside 968/466.0 from migmatites

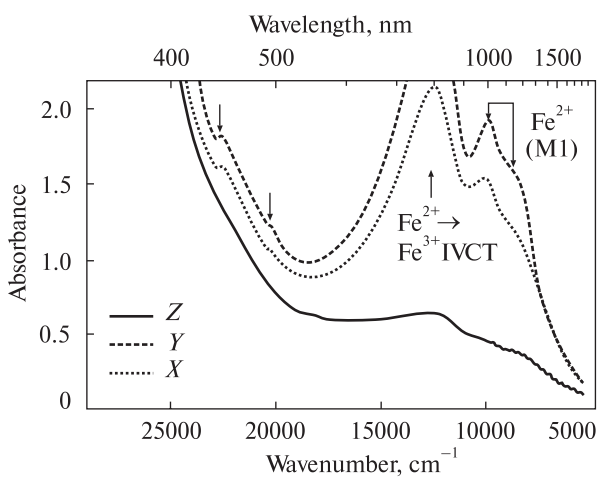


Fig. 4. Polarized absorption spectra of augite 741/278.5-1 from fenitized syenite

microscope REMMA-202M with energy dispersive spectrometer (EDS) as described by Yurchenko et al. [12]. Polarized optical absorption spectra in the range of 350–1800 nm ( $\sim 28600$ – $5560$   $\text{cm}^{-1}$ ) were measured on the automated home-made computer-controlled single-beam spectrophotometer constructed on the basis of monochromator Spectra-Pro-275 and highly modified polarizing microscope MIN-8 accomplished with photometric device and three changeable photo-detectors. More detailed description of the installation and the procedure of the single-beam spectra registration can be found, for instance, in Taran et al. [30].

Suitable for optical spectroscopic studies petrographic thin sections, standard and polished, i.e. not covered by glass slides, have been prepared from the clinopyroxene containing rocks. Orientation of clinopyroxene crystal grains was deter-

mined on the universal stage. As a result, sufficiently large (up to 0.2 mm across) clinopyroxene grains close to (010), i.e. of optical orientation, which allows measuring of optical absorption spectra in polarizations  $\sim E||X$  and  $\sim E||Z$  (the deviation from the exact orientation in all cases did not exceed  $10^\circ$ ), have been chosen for spectroscopic measurements. Herewith *a priori* is considered that all thin sections and, thus, the all pyroxene grains in them were of equal thickness.

The CIE colorimetric characteristics of the pyroxenes studied were calculated using Spectral Calculator Spreadsheets for  $\Delta\lambda = 5$  nm\*. For that the optical transmission spectra were recalculated to the spectral range 340–830 nm with the step  $\Delta\lambda = 5$  nm using Un-Scan-It 6.0 software.

Samples of apatite-containing fenitized pyroxenites (well 834), fenites and fenitized schists (well 741) have been selected in the area where carbonated fenites and melanocratic metasomatic rocks occur (Fig. 2, Tab. 1). Samples of fenite, formed by replacement of biotite-clinopyroxene schist, were taken from the area of alkaline and nepheline syenites (well 966). Outside the fenite halo samples of clinopyroxene-amphibole migmatite of granite composition, migmatite of tonalite composition and migmatite of granosyenite composition have been selected (well 968).

**Results and Discussion.** In polarized optical spectra of the calcic clinopyroxenes studied (Table 2) the aforementioned spectroscopic features, typical of natural iron containing clinopyroxenes related to both individual "isolated"  $\text{Fe}^{2+}$  and  $\text{Fe}^{3+}$  ions and their interaction (IVCT  $\text{Fe}^{2+} \rightarrow \text{Fe}^{3+}$  transitions) are observed. For instance, Fig. 3 and 4 show the spectra of two clinopyroxenes, 968/466.0-1 and 741/278.5-1, respectively, from two different wells, 968 and 741. As can be seen from the Figures, the spectra differ significantly from each other, first of all, by the intensity of all main spectroscopic features that is apparently due to differences in iron contents (cf. Tab. 2). In both cases a high-energy absorption edge, interpreted as a long-wave "tail" of the intense UV absorption bands caused by electronic ligand-metal charge-transfer transitions of  $\text{O}^{2-} \rightarrow \text{Fe}^{3+}$  and  $\text{O}^{2-} \rightarrow \text{Fe}^{2+}$  type, dominates in high-energy range of the spectra in all three polarizations. Together with a broad intense pleochroic  $\text{Fe}^{2+} \rightarrow \text{Fe}^{3+}$  IVCT band ( $Z \geq Y \geq X$ ) with maxima, depending on the polarization, from ca.

\* <http://www.bruceindbloom.com/index.html?SpectralCalcSpreadsheets.html>

12 500 to 12 900  $\text{cm}^{-1}$ , it forms a broad "window" of transparency and causes appearance of blue-green, green and brownish colorations of the pyroxenes. As seen from the spectra exemplified in Figures 3 and 4, the intensity ratio of Z- and X-polarized components of the IVCT band may significantly differ in pyroxenes of different composition. Most likely, this is due to change of orientation (rotation) of optical indicatrix axes Z and X round to the crystallographic axes *a* and *c* [10]. Thus, in the ferrian augite (augite-diopside) from migmatite of tonalite composition (Fig. 3) these bands have nearly equal intensities in all three polarizations, while in the spectrum of aluminian augite from fenitized syenite (Fig. 4) the intensity of this band in X-polarization is almost six times higher than in polarization Z (for Y-polarization this ratio is even higher, but cannot be exactly determined at a thickness of the actual thin section: the  $\text{Fe}^{2+} \rightarrow \text{Fe}^{3+}$  IVCT absorption band is so intense that in X-polarization in the wavelength range from  $\sim 720$  nm to  $\sim 850$  nm the sample becomes practically non-transparent).

Indeed, optical absorption value  $D = \lg \frac{I_0}{I}$ , where

$I_0$  and  $I$  is the intensity of the monochromatic light falling on and passed through the sample, respectively, exceeds in this range the value 2.0. This means that more than 99 % of irradiation is totally absorbed.

Note that according to Table 2, the iron content in pyroxenes 741/278.0-1 is nearly three times higher than in pyroxenes 968/466.0-1. However this difference can hardly be the only reason of different intensity of the  $\text{Fe}^{2+} \rightarrow \text{Fe}^{3+}$  IVCT and aforementioned near-infrared bands in Fig. 3 and 4, caused by spin-allowed electronic dd-transitions of  $\text{Fe}^{2+}$  in octahedral M1 and M2 positions of the structure. Along with much more intense short-wave absorption edge this indicates a relatively high concentration of  $\text{Fe}^{3+}$  ions and thus suggests that the oxidation state of iron in pyroxenes 741/278.0-1 must be appreciably higher than in 968/466.0-1. That means that the electronic exchange interaction between  $\text{Fe}^{2+}$  and  $\text{Fe}^{3+}$  also contribute the intensity of spin-allowed bands of  $\text{Fe}^{2+}$  (M1, M2) [24, 25], although these deduction does not much agree with calculated  $\text{Fe}^{3+}$ -content in the samples in question (Tab. 2). This shows that because of a low precision and relatively high limits of detection, semi-quantitative EDS method allows only rough estimations of chemical composition of such complex minerals as pyroxenes. Precise evaluation of iron valence state would probably require more accurate mea-

surements, for instance by means of the wavelength dispersive mode (WDS). A similar conclusion can be drawn from comparison of other pyroxene spectra, e. g. 741/278.0-1 and 966/573.0-3 or 966/573.0-6, where the difference in Fe-content between them is not so large as in the above mentioned samples 741/278.0-1 and 968/466.0-1 (Table 2). It should be noted that in this case using of other spectroscopic methods, such as Mössbauer spectroscopy allowing to evaluate the oxidation level of iron, is strongly restricted because of very small dimension of the pyroxenes grains and, especially, of their fine intergrowth with mica and amphiboles.

In most of the samples studied here the spectrum in Y-polarization by its general configuration does not significantly differ from the spectra in the two other polarizations: X and Z, as in Fig. 4. Therefore, a lack of an intense and clearly distinct Y-polarized absorption band of  $\text{Fe}^{2+}$  (M2) in the most samples studied indicates that M2 positions in them are completely filled by  $\text{Ca}^{2+}$  and  $\text{Na}^{+}$  ions and, thus,  $\text{Fe}^{2+}$  is concentrated in the M1-site despite of the fact that for some samples microprobe analysis indicates a deficiency of  $\text{Ca}^{2+}$  and  $\text{Na}^{+}$  (Tab. 2). Only in Y-polarized spectrum of a few samples a relatively intense broad band appears in the region  $\sim 9800$   $\text{cm}^{-1}$ . With a weaker band at  $\sim 4400$   $\text{cm}^{-1}$  in X-polarization (out of the spectral range studied here) it forms a strongly split doublet caused by electronic spin-allowed  ${}^5T_{2g} \rightarrow {}^5E_g$  transition of  $\text{Fe}^{2+}$  in a low symmetric cationic position M2 [16, 21, 9]. Such situation is seen in Fig. 3 (band in Y-polarization, marked as  $\text{Fe}^{2+}$  (M2)).

Selective absorption of white light illumination, which in fact is an equilibrated mixture of the visible monochromatic radiations of different wavelengths [3], by the short-wave absorption edge and  $\text{Fe}^{2+} \rightarrow \text{Fe}^{3+}$  IVCT band, causes coloration of pyroxene grains in petrographic thin sections at their visual observation in transmitting illumination with a microscope. The variations in the shape and depth of the transparency window of differently oriented grains are perceived as pleochroism, especially distinct at observation in polarized light. Although quantification of color and pleochroism of clinopyroxenes in petrographic thin sections is considered to be most suitable in (100)-sections [10, 9], in this paper colorimetric characteristics were calculated from  $\sim E \parallel X$ - and  $\sim E \parallel Z$ -polarized spectra of the grains with the appropriate orientation. Visually at observation in polarized light they are characterized by a quite variable intensity

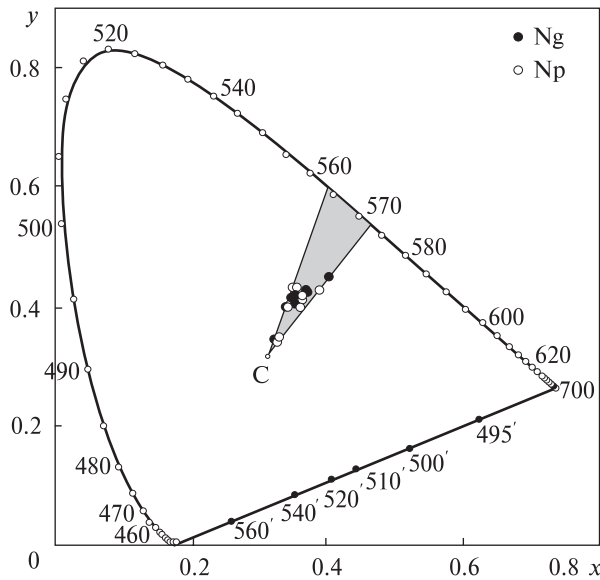


Fig. 5. Loci of thirteen grains of clinopyroxenes with orientation in the sections close to (010) and calculated from Z- and X-polarized optical transmission spectra in relation to the standard illuminant C on the chromaticity diagram of CIE colorimetric system. The values of the wavelength of the primary color  $\lambda_k$  are in quite a narrow range of 564 to 572 nm (filled in with gray color)

of color and, for some weakly oxidized varieties, of mild pleochroism from yellow-green in Z- to a rich green in X-polarization.

It should be noted that since color is inherently three-dimensional quantity (trichromatic), any colorimetric system requires three coordinates for its description. Therefore, its graphical representation as two-dimensional Figures is always a certain simplification of the situation. In the CIE colorimetric system, the most common is the graphical representation of colors in the chromaticity diagram wherein such color characteristics as the dominant color wavelength  $\lambda_k$  and its purity or saturation  $p_c$  may be evaluated [2, 3].

In Table 3 the color characteristics  $\lambda_k$ ,  $p_c$  and Y calculated from Z- and X-polarized spectra of the pyroxenes studied are compiled, whereas the locus's of the samples on the standard chromaticity diagram of CIE colorimetric system are shown in Figure 5. According to the Table and Figure, the  $\lambda_k$  values are located in quite a narrow range from 564 to 572 nm. For the samples which spectra have been measured in polarization close to Y, the calculated  $\lambda_k$ -values are also in this range. In other words, by the tonality variations the pleochroism of the pyroxenes studied may be characterized as relatively weak. The difference in color in different polarizations is mostly related to changes in Y- and  $p_c$ -values. The former expectedly increases with increase of iron content and the degree of its

Table 3. Values of color characteristics  $\lambda_k$  (wavelength of the dominant color),  $p_c$  (dominant color purity or saturation) and Y (luminance) for clinopyroxene grains in the sections close to (010) in petrographic thin sections expressed in CIE colorimetric system calculated from Z- and X-polarized optical transmission spectra in relation to the standard illuminant C

Sample	Polarization					
	Z			X		
	$\lambda_k$ , nm	$p_c$ , rel. units	Y, %	$\lambda_k$ , nm	$p_c$ , rel. units	Y, %
834-1/250.41	568.0	0.422	29.5	564.1	0.420	29.8
741-1/243.0-12	569.0	0.461	19.8	565.5	0.436	21.1
741-1/243.0-23	568.1	0.417	15.3	566.1	0.422	19.1
741-1/246.04	568.0	0.374	33.8	566.0	0.349	39.3
741-1/278.55	572.1	0.614	26.2	569.9	0.354	39.1
741-1/287.0-16	569.0	0.435	36.6	564.2	0.407	28.0
741-1/287.0-27	568.2	0.383	52.2	564.1	0.361	43.3
741-1/306.98	568.9	0.383	42.9	564.2	0.375	32.0
966/573.0-19	568.9	0.365	41.8	566.0	0.342	43.1
966/573.0-210	568.3	0.391	26.3	568.1	0.395	27.3
968/453.811	564.1	0.101	82.6	566.0	0.115	78.8
968/466.012	567.2	0.155	50.0	568.0	0.139	52.0
968/472.013	564.8	0.322	81.1	564.1	0.311	80.0

Note. 1 – hedenbergite; 2, 3 – augite; 4 – aluminian augite; 5 – ferrian, sodian augite; 6, 7 – aluminian, sodian augite; 8 – aluminian sodian augite; 9, 10 – sodian diopside; 11 – ferrian diopside; 12 – ferrian augite (augite-diopside); 13 – augite.



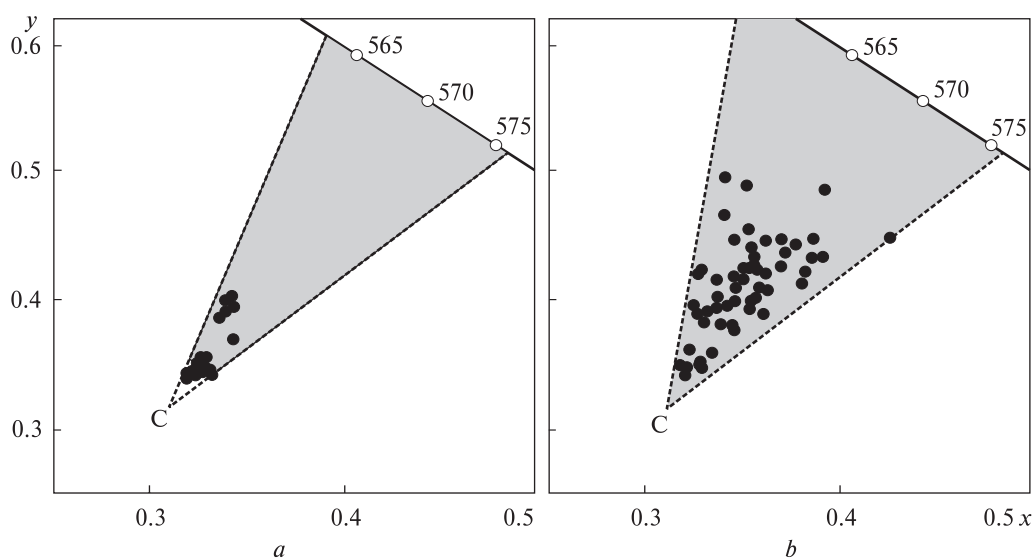


Fig. 6. The fragments of the chromaticity diagram CIE with loci of pyroxenes from the wells 968 (a) and 741 (b)

oxidation what, as already noted, leads to the shift of the short-wavelength absorption edge to the visible range on the one hand and the intensification of  $\text{Fe}^{2+} \rightarrow \text{Fe}^{3+}$  IVCT band, and, accordingly, increase of absorption in the red part of the visible range, on the other hand. As a result, it makes the transmittance window deeper and narrower and the color more saturated ( $p_c$  is increasing) and darker ( $Y$  is decreasing). This is particularly clear when compare color parameters of pale-green augites from crystalline rocks of the eastern (lying) block of Chernihivka zone (well 968) or augites-malacolites from fenitized rocks of the western block (well 966) and dark-green sodium-iron augites and aluminian sodian augites from metamorphically altered rocks of the central block of Chernihivka fault zone (well 741). Fig. 6, *a* and Fig. 6, *b* show the examples of the chromaticity diagram fragments and the loci calculated from the unpolarized spectra of randomly oriented grains of clinopyroxenes in the thin sections of the rocks from the wells 968 and 741, respectively. Apparently, in the first case chromaticity of pyroxenes is characterized by low  $p_c$ -values (is located close to the point C, which is the locus of the standard illuminant C imitating a white diffuse day-light). This indicates a low saturation of the dominant color with the wavelength  $\lambda_k$  in the range of 562.5 to 574.1 nm. The pyroxenes from the well 741 are characterized by much wider range of the  $\lambda_k$ -values

from 556.5 to 576 nm and broader range of the  $p_c$ -values ranging from 0.09 to 0.68. The luminance  $Y$ -values, as seen from the Table 3, are much higher for pyroxenes from the well 968 than those from the well 741.

**Conclusions.** Thus, according to our study, the color of clinopyroxenes from fenitized rocks of Chernihivka carbonatite massif is caused by presence of  $\text{Fe}^{2+}$  and  $\text{Fe}^{3+}$  ions in the structure. Concentrations of other transition metal ions, according to microprobe analysis data, are significantly lower and do not much influence the spectroscopic and color characteristics. The character of polarized absorption spectra in the near-infrared region indicates that  $\text{Fe}^{2+}$  occupies mainly the structural cationic position M1, thus showing that another position, M2, which can also accommodate  $\text{Fe}^{2+}$ , is almost completely filled with ions of calcium and sodium. The nature of color and pleochroism of pyroxenes in X-, Y- and Z-polarizations are caused by both the iron content and the degree of its oxidation and mutual orientation of Y and Z axes relating to crystallographic axes  $a$  and  $c$  in pyroxenes of different compositions. The position of color points of the pyroxenes studied in the chromaticity diagram XYZ is different for the samples from different wells indicating different coloration which, in its turn, is caused by both different iron content and different  $\text{Fe}^{2+}$  and  $\text{Fe}^{3+}$  concentration ratios.

## REFERENCES

1. Glevasskiy, E.B. and Kryvdik, S.G. (1981), *Dokembriyskiy karbonatitoviy kompleks Priazovya*, Nauk. dumka, Kyiv, UA, 228 p.
2. Gurevich, M.M. (1950), *Tsvet i ego izmerenie*, Izd-vo AN SSSR, Moscow, RU, 283 p.
3. Judd, D. and Wysecki, G. (1978), *Color in Business, Science, and Industry*, Mir, Moscow, RU, 592 p.
4. Matsyuk, S.S., Platonov, A.N. and Khomenko V.M. (1985), *Opticheskie spektry i okraska mantijnykh mineralov v kimberlitah*, Nauk. dumka, Kyiv, UA, 248 p.
5. Nikanorova, Yu.Ye., Lazaryeva, I.I., Shnyukov, S.Ye. and Kovtun, O.V. (2015), *Mineralni resursy Ukrainy*, No. 1, Kyiv, UA, pp. 20-26.
6. Platonov, A.N., Taran, M.N. and Balitsky, V.S. (1984), *Priroda okraski samotsvetov*, Nedra, Moscow, RU, 196 p.
7. Rusakov, N.F. and Kravchenko, G.L. (1986), *Geological journal*, Vol. 46, No. 4, Kyiv, UA, pp. 112-118.
8. Taran, M., Yurchenko, N. and Shnyukov, S. (2014), *Mineral. zbirnyk*, No. 64, Iss. 2, Lviv, UA, pp. 95-103.
9. Khomenko, V.M. (2015), *Mineral. Journ. (Ukraine)*, Vol. 37, No. 3, Kyiv, UA, pp. 15-27.
10. Khomenko, V.M. and Platonov, A.N. (1987), *Porodoobrazuyushchie pirokseny: opticheskie spektry, okraska i pleokhroizm*, Nauk. dumka, Kyiv, UA, 214 p.
11. Shestopalov, D.I., Golubeva, L.F., Taran, M.N. and Khomenko, V.M. (1991), *Astromiicheskiy vestnik*, Vol. 25, No. 4, pp. 442-452.
12. Shcherbak, N.P., Zlobenko, V.G., Zhukov, G.V., Kotlovskaya, F.I., Polevaya, N.I., Komlev, L.V., Kovalenko, N.K., Nosok, G.M. and Pochtarenko, V.I. (1978), *Katalog izotopnykh dat porod Ukrainskogo shchita*, Nauk. dumka, Kyiv, UA, 224 p.
13. Shcherbakov, I.B. (2005), *Petrology of the Ukrainian Shield*, ZUKTS press, Lviv, UA, 366 p.
14. Yurchenko, N.G., Shnyukov, S.Ye. and Pavlov, G.G. (2015), *Mineral. zbirnyk*, No. 65, Iss. 1, Lviv, UA, pp. 84-94.
15. Amthauer, G., and Rossman, G.R. (1984), *Phys. Chem. Minerals*, Vol. 11 (2), pp. 37-51, doi: 10.1007/BF00309374.
16. Burns, R.G. (1993), *Mineralogical application of crystal field theory*, Cambr. Univ. Press, Cambridge, 550 p., doi: <http://dx.doi.org/10.1017/CBO9780511524899>
17. Cameron, M., Shigeo, S., Prewitt, C.T. and Papike, J.J. (1973), *Amer. Miner.*, Vol. 58 (7-8), pp. 594-618.
18. Cloutis, E.A. (2002), *J. Geophys. Res.*, Vol. 107 (E6), p. 5039, doi: <https://doi.org/10.1029/2001JE001590>
19. Klima, R.L., Pieters, C.M. and Dyar, M.D. (2007), *Meteoritics and Planet. Sci.*, Vol. 42, pp. 235-253, doi: <https://doi.org/10.1111/j.1945-5100.2007.tb00230.x>
20. Langer, K. and Khomenko, V.M. (1999), *Contribs Mineral. and Petrol.*, Vol. 137, pp. 220-223, doi: <https://doi.org/10.1007/s004100050547>
21. Marfunin, A.S. (1979), *Physics of Minerals and Inorganic Materials. An Introduction*, Springer Verlag, Berlin, Heidelberg, N-Y, 340 p.
22. Rossman, G.R. (1980), *Pyroxene spectroscopy*, in Prewitt, C.T. (ed.), *Pyroxenes, Revs Mineral. and Geochem.*, Vol. 7, pp. 93-115.
23. Rossman, G.R. (1988), *Spectroscopic Methods in Mineralogy and Geology*, in Hawthorne, F.C. (ed.), *Revs. Mineral.*, Vol. 18, pp. 207-254.
24. Skogby, H., Hälenius, U., Kristiansson, P. and Ohashi, H. (2006), *Amer. Miner.*, Vol. 91 (11-12), pp. 1794-1801, doi: <https://doi.org/10.2138/am.2006.2154>
25. Smith, G. (1978a), *Phys. Chem. Minerals*, Vol. 3 (4), pp. 343-373, doi: <https://doi.org/10.1007/BF00311847>
26. Smith, G. (1978b), *Phys. Chem. Minerals*, Vol. 3 (4), pp. 375-383, doi: <https://doi.org/10.1007/BF00311848>
27. Straub, D.W., Burns, R.G. and Pratt, S.F. (1991), *Geophys. Res.*, Vol. 96, pp. 18819-30, doi: <https://doi.org/10.1029/91JE01893>
28. Taran, M.N., Ohashi, H., Langer, K. and Vishnevskyy, A.A. (2011), *Phys. Chem. Minerals*, Vol. 38 (5), pp. 345-356, doi: [10.1007/s00269-010-0408-x](https://doi.org/10.1007/s00269-010-0408-x)
29. Taran, M.N. and Langer, K. (2001), *Phys. Chem. Minerals*, Vol. 28 (3), pp. 199-210, doi: [10.1007/s002690000148](https://doi.org/10.1007/s002690000148)
30. Taran, M.N., Ohashi, H. and Koch-Müller, M. (2008), *Phys. Chem. Minerals*, Vol. 35 (3), pp. 117-127, doi: [10.1007/s00269-007-0202-6](https://doi.org/10.1007/s00269-007-0202-6)

Received 06.08.2018

## ЛІТЕРАТУРА

1. Глевасский Е.Б., Кривдик С.Г. Докембрийский карбонатитовый комплекс Приазовья. — Киев : Наук. думка, 1981. — 228 с.
2. Гуревич М.М. Цвет и его измерение. — М. : Изд-во АН СССР, 1950. — 283 с.
3. Джадд Д., Вышецки Г. Цвет в науке и технике. — М. : Мир, 1978. — 592 с.
4. Мацюк С.С., Платонов А.Н., Хоменко В.М. Оптические спектры и окраска мантийных минералов в кимберлитах. — Киев : Наук. думка, 1985. — 248 с.
5. Никанорова Ю.Є., Лазарева І.І., Шнюков С.Є., Ковтун О.В. Карбонатитові комплекси центрального та лінійного структурно-морфологічного типів: співставлення фенітових ореолів на прикладі масивів Альньо (Швеція) та Чернігівського (Україна) // Мінеральні ресурси України. — 2015. — № 1. — С. 20—26.

6. Платонов А.Н., Таран М.Н., Балицкий В.С. Природа окраски самоцветов. — М. : Недра, 1984. — 196 с.
7. Русаков Н.Ф., Кравченко Г.Л. К вопросу о структуре Черниговского массива карбонатитов (Приазовье) // Геол. журн. — 1986. — 46, № 4. — С. 112—118.
8. Таран М., Юрченко Н., Шнюков С. Биотит кристалічних порід Новополтавської ділянки Чернігівської зони розлому (Західне Приазов'я) // Мінерал. зб. — 2014. — № 64, вип. 2. — С. 95—103.
9. Хоменко В.М. Кристалохімія та спектроскопія егірінів Октябрського масиву та лужних метасоматитів Приазов'я // Мінерал. журн. — 2015. — 37, № 3. — С. 15—27.
10. Хоменко В.М., Платонов А.Н. Пороодообразующие пироксены: оптические спектры, окраска и плеохроизм. — Киев : Наук. думка, 1987. — 214 с.
11. Шестопалов Д.И., Голубева Л.Ф., Таран М.Н., Хоменко В.М. Полосы поглощения железа и хрома в спектрах земных пироксенов: применение к дистанционному минералогическому анализу поверхности астероидов // Астрономич. вестник. — 1991. — 25, № 4. — С. 442—452.
12. Щербак Н.П., Злобенко В.Г., Жуков Г.В., Котловская Ф.И., Полевая Н.И., Комлев Л.В., Коваленко Н.К., Носок Г.М., Почтаренко В.И. Каталог изотопных дат пород Украинского щита. — Киев : Наук. думка, 1978. — 224 с.
13. Щербак И.Б. Петрология Украинского щита. — Львов : ЗУКЦ, 2005. — 366 с.
14. Юрченко Н., Шнюков С., Павлов Г. Нові дані щодо хімічного складу піроксенів з фенітів Чернігівського карбонатитового масиву (Західне Приазов'я, Український щит) // Мінерал. зб. — 2015. — № 65, вип. 1. — С. 84—94.
15. Amthauer G., Rossman G.R. Mixed valence of iron in minerals with cation clusters // Phys. Chem. Minerals. — 1984. — 11 (2). — P. 37-51, doi: <https://doi.org/10.1007/BF00309374>
16. Burns R.G. Mineralogical application of crystal field theory. — Cambridge : Cambridge Univ. Press, 1993. — 2nd edition. — 550 p., doi: <http://dx.doi.org/10.1017/CBO9780511524899>
17. Cameron M., Shigeho S., Prewitt C.T., Papike J.J. High-temperature crystal chemistry of acmite, diopside, hedenbergite, jadeite, spodumene, and ureyite // Amer. Miner. — 1973. — 58 (7—8). — P. 594—618.
18. Cloutis E.A. Pyroxene reflectance spectra: Minor absorption bands and effects of elemental substitutions // J. Geophys. Res. — 2002. — 107 (E6). — P. 5039, doi: <https://doi.org/10.1029/2001JE001590>
19. Klima R.L., Pieters C.M., Dyar M.D. Spectroscopy of synthetic Mg-Fe pyroxenes I: Spin-allowed and spin-forbidden crystal field bands in the visible and near-infrared // Meteoritics and Planet. Sci. — 2007. — 42. — P. 235—253, doi: <https://doi.org/10.1111/j.1945-5100.2007.tb00230.x>
20. Langer K., Khomenko V.M. The influence of crystal field stabilization energy on Fe<sup>2+</sup> partitioning in paragenetic minerals // Contribs Mineral and Petrol. — 1999. — 137. — P. 220—223, doi: <https://doi.org/10.1007/s004100050547>
21. Marfunin A.S. Physics of Minerals and Inorganic Materials. An Introduction. — Springer Verlag, Berlin, Heidelberg, N-Y, 1979. — 340 p.
22. Rossman G.R. Pyroxene spectroscopy / Ed. C.T. Prewitt, Pyroxenes // Revs Miner. — 1980. — 7. — P. 93—115.
23. Rossman G.R. Optical spectroscopy // Spectroscopic Methods in Mineralogy and Geology / Ed. F.C. Hawthorne // Revs Miner. — 1988. — 18. — P. 207—254.
24. Skogby H., Hälenius U., Kristiansson P., Ohashi H. Titanium incorporation and <sup>VI</sup>Ti<sup>3+</sup> — <sup>IV</sup>Ti<sup>4+</sup> charge transfer in synthetic diopside // Amer. Miner. — 2006. — 91 (11—12). — P. 1794—1801, doi: <https://doi.org/10.2138/am.2006.2154>
25. Smith G. A reassessment of the role of iron in the 5.000—30.000 cm<sup>-1</sup> region of the electronic absorption spectra of tourmaline // Phys. Chem. Minerals. — 1978. — 3 (4). — P. 343—373, doi: <https://doi.org/10.1007/BF00311847>
26. Smith G. Evidence for absorption by exchange-coupled Fe<sup>2+</sup>-Fe<sup>3+</sup> pairs in the near infra-red spectra of minerals // Phys. Chem. Minerals. — 1978. — 3 (4). — P. 375—383, doi: <https://doi.org/10.1007/BF00311848>.
27. Straub D.W., Burns R.G., Pratt S.F. Spectral signature of oxidized pyroxenes: Implications to remote-sensing of terrestrial planets // Geophys. Res. — 1991. — 96. — P. 1889-30, doi: <https://doi.org/10.1029/91JE01893>
28. Taran M.N., Ohashi H., Langer K., Vishnevskyy A.A. High-pressure electronic absorption spectroscopy of natural and synthetic Cr<sup>3+</sup>-bearing clinopyroxenes // Phys. Chem. Minerals. — 2011. — 38 (5). — P. 345—356, doi: <https://doi.org/10.1007/s00269-010-0408-x>
29. Taran M.N., Langer K. Electronic absorption spectra of Fe<sup>2+</sup> ions in oxygen-based rock-forming minerals at temperatures between 297 and 600 K // Phys. Chem. Minerals. — 2001. — 28 (3). — P. 199—210, doi: <https://doi.org/10.1007/s002690000148>.
30. Taran M.N., Ohashi H., Koch-Müller M. Optical spectroscopic study of synthetic NaScSi<sub>2</sub>O<sub>6</sub> — CaNiSi<sub>2</sub>O<sub>6</sub> pyroxenes at normal and high pressures // Phys. Chem. Minerals. — 2008. — 35 (3). — P. 117—127, doi: <https://doi.org/10.1007/s00269-007-0202-6>

Надійшла 06.08.2018

*Н.Г. Юрченко, М.М. Таран*

Институт геохимии, минералогии та рудоутворення  
ім. М.П. Семененка НАН України  
03142, м. Київ, Україна, пр-т Акад. Палладіна, 34  
E-mail: Nadysya88@gmail.com, m\_taran@hotmail.com

#### ОПТИКО-СПЕКТРОСКОПИЧНЕ І КОЛОРИМЕТРИЧНЕ ВИВЧЕННЯ ПІРОКСЕНІВ ІЗ ФЕНІТИЗОВАНИХ ПОРІД ЧЕРНІГІВСЬКОГО КАРБОНАТИТОВОГО МАСИВУ ПРИАЗОВ'Я

У дослідженні карбонатитових комплексів головну увагу приділено вивченню саме карбонатитів та пов'язаних із ними різноманітних силікатних магматичних порід, тоді як породам ореолів фенітизації, які завжди супроводжують карбонатитові комплекси і є потужним пошуковим критерієм, приділяють значно менше уваги. Для розширення засобів прогнозування та пошуку карбонатитів у межах Українського щита досліджено вплив лужних фенітизувальних розчинів на спектроскопічні параметри, характер забарвлення і плеохроїзм породоутворювальних мінералів. У цій роботі представлені результати оптико-спектроскопічного і колориметричного вивчення піроксенів із метасоматично змінених клінопіроксенітів, кристалічних сланців, піроксенвмісних мигматитів гранітового, тоналітового та граносієнітового складу, сієнітів та лужних сієнітів фенітового ореолу північної ділянки розповсюдження чернігівського карбонатитового комплексу та із незмінених вмісних порід його гнейсово-мигматитової рами. Встановлено, що спектроскопічні характеристики, забарвлення і плеохроїзм піроксенів зумовлені присутністю та співвідношенням у кристалічній структурі різновалентних іонів заліза  $Fe^{2+}$  і  $Fe^{3+}$ , які зумовлюють появу смуг поглинання кристалічного поля (смуг електронних  $dd$ -переходів) і смуг переносу заряду  $Fe^{2+} \rightarrow Fe^{3+}$ . Було виявлено, що позиція  $M2$  в досліджених клінопіроксенах майже повністю заповнена іонами кальцію та натрію у той час, як іони  $Fe^{2+}$  в основному займають структурну катіонну позицію  $M1$ . Тим не менше, навіть відносно невелика частка іонів  $Fe^{2+}(M2)$  суттєво впливає на характер оптичного поглинання у ближній інфрачервоній області. Колориметричне дослідження зерен піроксену з деяких порід ореолу фенітизації дало змогу визначити різний характер забарвлення та насиченості, що обумовлено різним вмістом заліза і ступенем його окиснення.

*Ключові слова:* Український щит, Чернігівський карбонатитовий масив, фенітовий ореол, піроксени, оптична спектроскопія, колориметричні дослідження.

*Н.Г. Юрченко, М.Н. Таран*

Институт геохимии, минералогии и рудообразования  
им. Н.П. Семененко НАН Украины  
03142, г. Киев, Украина, пр-т Акад. Палладина, 34  
E-mail: Nadysya88@gmail.com, m\_taran@hotmail.com

#### ОПТИКО-СПЕКТРОСКОПИЧЕСКОЕ И КОЛОРИМЕТРИЧЕСКОЕ ИССЛЕДОВАНИЕ ПИРОКСЕНОВ ИЗ ФЕНИТИЗИРОВАННЫХ ПОРОД ЧЕРНИГОВСКОГО КАРБОНАТИТОВОГО МАССИВА ПРИАЗОВЬЯ

В исследованиях карбонатитовых комплексов главное внимание уделено изучению именно карбонатитов и связанных с ними различных силикатных магматических пород, тогда как породам ореолов фенитизации, всегда сопровождающим карбонатитовые комплексы и служащих мощным поисковым критерием, уделено значительно меньше внимания. Для расширения способов прогнозирования и поиска карбонатитов в пределах Украинского щита выполнено изучение влияния щелочных фенитизирующих растворов на спектроскопические параметры, характер окраски и плеохроизм породообразующих минералов. В этой работе представлены результаты оптико-спектроскопического и колориметрического изучения пироксенов из метасоматически измененных клинопироксенитов, кристаллических сланцев, пироксенсодержащих мигматитов гранитового, тоналитового и граносиєнітового состава, сиєнітов и щелочных сиєнітов фенитового ореола северного участка распространения черниговского карбонатитового комплекса и из неизмененных вмещающих пород его гнейсово-мигматитовой рамы. Установлено, что спектроскопические характеристики, окраска и плеохроизм пироксенов, обусловленные присутствием и соотношением в кристаллической структуре разновалентных ионов железа  $Fe^{2+}$  и  $Fe^{3+}$ , обуславливающих появление как полос поглощения кристаллического поля (полос электронных  $dd$ -переходов), так и полос переноса заряда  $Fe^{2+} \rightarrow Fe^{3+}$ . Было обнаружено, что позиция  $M2$  в исследованных клинопіроксенах почти полностью заполнена ионами кальция и натрия в то время, как ионы  $Fe^{2+}$ , в основном, занимают структурную катионную позицию  $M1$ . Тем не менее, даже относительно небольшая часть ионов  $Fe^{2+}(M2)$  существенно влияет на характер оптического поглощения в ближней инфракрасной области. Колориметрическое исследование зерен пироксена из некоторых пород ореола фенитизации дало возможность установить разный характер окраски и насыщенности, что обусловлено разным содержанием железа и степенью его окисления.

*Ключевые слова:* Украинский щит, Черниговский карбонатитовый массив, фенитовый ореол, пироксены, оптическая спектроскопия, колориметрические исследования.